

RESEARCH

Open Access



Taxonomy of the White-browed Shortwing (*Brachypteryx montana*) complex on mainland Asia and Taiwan: an integrative approach supports recognition of three instead of one species

Per Alström^{1,2,3*}, Pamela C. Rasmussen^{4,5}, Canwei Xia⁶, Magnus Gelang⁷, Yang Liu⁸, Guoling Chen⁸, Min Zhao^{3,9}, Yan Hao^{3,9}, Chao Zhao¹⁰, Jian Zhao⁸, Chengte Yao¹¹, James A. Eaton¹², Robert Hutchinson¹², Fumin Lei³ and Urban Olsson¹³

Abstract

Background: The White-browed Shortwing (*Brachypteryx montana*) is widespread from the central Himalayas to the southeast Chinese mainland and the island of Taiwan, the Philippines and Indonesia. Multiple subspecies are recognised, and several of these have recently been suggested to be treated as separate species based on differences in morphology and songs.

Methods: We here analyse plumage, morphometrics, songs, two mitochondrial and two nuclear markers, and geographical distributions of the two mainland Asian taxa *B. m. cruralis* and *B. m. sinensis* and the Taiwanese *B. m. goodfellowi*.

Results: We conclude that these differ congruently in morphology, songs and DNA. Male *B. m. goodfellowi* is the most divergent in plumage (sexually monomorphic, unlike the two others; male similar to female), and *B. m. cruralis* and *B. m. sinensis* differ in male plumage maturation. The song of *B. m. cruralis* is strongly divergent from the others, whereas the songs of *B. m. sinensis* and *B. m. goodfellowi* are more similar to each other. *Brachypteryx m. sinensis* and *B. m. goodfellowi* are sisters, with an estimated divergence time 4.1 million years ago (mya; 95% highest posterior distribution [HPD] 2.8–5.5 mya), and *B. m. cruralis* separated from these two 5.8 mya (95% HPD 4.1–7.5 mya). We also report notable range extensions of *B. m. sinensis* as well as sympatry between this taxon and *B. m. cruralis* in Sichuan Province, China. *Brachypteryx m. montana* from Java is found to be more closely related to Lesser Shortwing (*B. leucophrys*) and Rusty-bellied Shortwing (*B. hyperythra*) than to the mainland Asian and Taiwanese taxa.

Conclusion: Our data support a recent proposal to treat the three mainland Asian and Taiwanese taxa as three species, separate from *B. montana* sensu stricto: *B. cruralis* (central Himalayas to south central China and south Vietnam), *B. sinensis* (north central to southeastern part of mainland China) and *B. goodfellowi* (Taiwan Island).

Keywords: Integrative taxonomy, Morphology, Song, Miocene, Pliocene

*Correspondence: per.alstrom@ebc.uu.se

¹ Department of Ecology and Genetics, Animal Ecology, Evolutionary Biology Centre, Uppsala University, Norbyvägen 18D, 752 36 Uppsala, Sweden

Full list of author information is available at the end of the article



© The Author(s) 2018. This article is distributed under the terms of the Creative Commons Attribution 4.0 International License (<http://creativecommons.org/licenses/by/4.0/>), which permits unrestricted use, distribution, and reproduction in any medium, provided you give appropriate credit to the original author(s) and the source, provide a link to the Creative Commons license, and indicate if changes were made. The Creative Commons Public Domain Dedication waiver (<http://creativecommons.org/publicdomain/zero/1.0/>) applies to the data made available in this article, unless otherwise stated.

Background

The genus *Brachypteryx* belongs to the family Muscicapidae, within which it has been suggested to be sister to the recently reinstated genus *Larvivora* (Sangster et al. 2010; Zuccon and Ericson 2010). Three species are usually recognised in *Brachypteryx* (White-browed Shortwing *B. montana*, Lesser Shortwing *B. leucophrys*, Rusty-bellied Shortwing *B. hyperythra*; Dickinson and Christidis 2014; Gill and Donsker 2018), although 10 species are recognised by del Hoyo and Collar (2016) (see below). Previously, Gould's Shortwing (*Heteroxenicus stellatus*) was also placed in *Brachypteryx*, but it was recently moved to a monotypic genus because of its distinct plumage and song (Collar 2005; Rasmussen and Anderton 2005; Dickinson and Christidis 2014; del Hoyo and Collar 2016; Gill and Donsker 2018), and a multilocus phylogenetic analysis has shown *Heteroxenicus* to be only distantly related to *Brachypteryx* (Price et al. 2014). Also two Indian Western Ghats endemics recently placed in the new genus *Sholicola* (*S. major*, *S. albiventris*) in the flycatcher subfamily Niltavinae based on molecular data (Robin et al. 2017) were previously often placed in *Brachypteryx*.

The White-browed Shortwing (*Brachypteryx montana*) occurs in montane regions from Nepal to southeastern mainland China and northwest Thailand and southern Vietnam, and on Taiwan Island and several of the islands in the Philippines and Indonesia (Fig. 1; continental Asian and Taiwan range). Fourteen subspecies are usually recognised (Collar 2005; Dickinson and Christidis 2014; Clement and Rose 2015; Gill and Donsker 2018). Most of the taxa are sexually dimorphic, with males being mainly blue-grey with a white supercilium, which is usually mostly concealed but which can be prominently displayed when agitated, and with mostly brown females (Collar 2005; Clement and Rose 2015).

Based on morphological and vocal characteristics, Eaton et al. (2016) split the Indonesian taxa into four species, and del Hoyo and Collar (2016) split the entire complex into eight allo-/parapatric species. For example, the latter authors treated the Himalayan and central Chinese *B. m. cruralis*, the southeast Chinese *B. m. sinensis* and the Taiwanese *B. m. goodfellowi* as specifically distinct from each other as well as from the Philippine and Indonesian taxa based on morphology and song. Based on two mitochondrial genes and one Z-linked region,

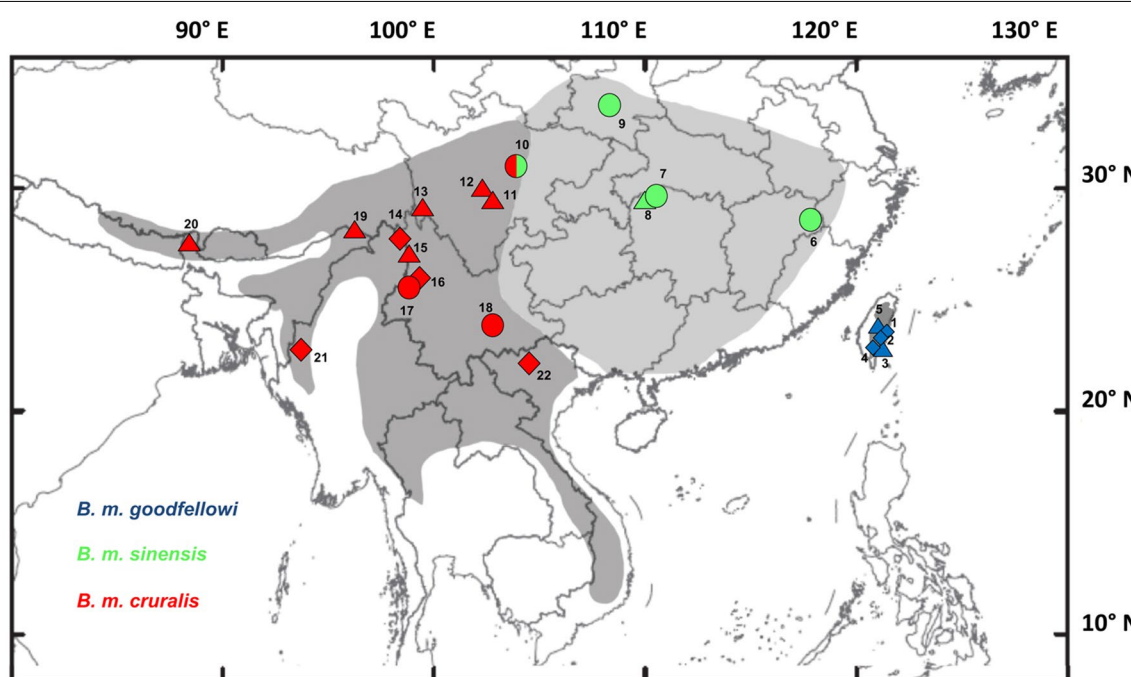


Fig. 1 Distribution of the continental and Taiwan Island *Brachypterus montana* complex (shaded areas), with sampling localities represented by circles (songs and DNA), diamonds (DNA) and triangles (song), and different colours for different taxa. The bicoloured circle represents a locality where *B. m. cruralis* and *B. m. sinensis* have been found in sympatry. Localities: 1. Hualien, Taiwan Island; 2. Nantou, Taiwan Island; 3. Sianyang Forest Resort, Taiwan Island; 4. Kaohsiung, Taiwan Island; 5. Dasyeushan Forest Resort, Taiwan Island; 6. Wuyishan, Jiangxi; 7. Hupingshan, Hunan; 8. Badagongshan, Hunan; 9. Foping, Shaanxi; 10. Wolong, Sichuan; 11. Longcanggou, Sichuan; 12. Labahe, Sichuan; 13. Muli, Sichuan; 14. Dulongjiang, Yunnan; 15. Pianma, Yunnan; 16. Dali, Yunnan; 17. Baihualing, Yunnan; 18. Huanglianshan, Yunnan; 19. Eaglenest; 20. Singalila National Park, West Bengal; 21. Chin Hills, Chin State; 22. Mucang Chai District, Yen Bou

Kyriazis et al. (2018) found deep divergence between the Sundaic and Philippine lineages versus mainland Asian *cruralis* and *sinensis*. Their analysis also suggested that the latter two taxa are deeply diverged from each other.

We here review the taxonomic status of the two taxa in this complex that occur on the Asian continent (*B. m. cruralis* and *B. m. sinensis*) and the single one that occurs on Taiwan Island (*B. m. goodfellowi*; Fig. 1). We do this by integrating plumage, morphometrics, song and mitochondrial and nuclear DNA, in addition to geographical distributions. We conclude that all three taxa are more appropriately treated as separate species.

Methods

Throughout the paper, we follow the traditional taxonomy, treating the three focal taxa as subspecies of *Brachypteryx montana* (Collar 2005; Dickinson and Christidis 2014; Clement and Rose 2015; Gill and Donsker 2018).

Morphology

Specimens of *B. m. cruralis*, *B. m. sinensis* and *B. m. goodfellowi* were examined by P.C.R. at the following museums: American Museum of Natural History, New York, USA (AMNH); Museum of Comparative Zoology, Cambridge, Massachusetts, USA (MCZ); the Natural History Museum, Tring, UK (NHMUK, formerly BMNH); National Museum of Natural History, Smithsonian Institution, Washington, D.C., USA (NMNH, specimen acronym USNM); and University of Michigan Museum of Zoology, Ann Arbor, USA (UMMZ). All available specimens at these museums of *B. m. sinensis* and *B. m. goodfellowi* were measured, while most of them including *B. m. cruralis* were measured at UMMZ. All museum specimens of *B. m. sinensis* available were from Fujian Province, China, i.e. not near the zone of contact discussed herein. Plumages were also studied, and documented by photographs, of all birds caught in the field.

Specimens were measured for 19 characters: culmen length (from skull base); culmen length (from distal feathers); bill width (from distal narial edge); bill depth (from distal narial edge); flattened wing (wing chord); secondary length (from bend of wing to tip of longest secondary); primary projection beyond longest secondary; length of Primary 1 (P1; numbered ascendantly beyond primary coverts; shortfalls from folded wingtip (longest primary) of primaries 1–5; tail length (with calipers inserted between middle two rectrices); tail graduation (distance from central to outermost rectrices in folded tail); tarsus length; tarsus distal width; and hind-claw length. Univariate statistics were generated and tested for equality of means where sample sizes permitted using two-sample *t*-tests with pooled variances,

Bonferroni-adjusted to control for Type I error, using MyStat (SYSTAT Software, Crane Software International, Ltd.). Available sample size of specimens of *B. m. goodfellowi* was too small for statistical analysis. A Principal Components Analysis (PCA) was done on the same set of external measurements (except carpal joint to longest secondary length and distal tarsal width, for which several specimens were not measured), using a covariance matrix in MyStat. Sexes were analyzed separately, and older, largely unspotted juveniles were included with the respective sex. Sexing was straightforward due to the presence of a white eyebrow in males, except in *B. m. goodfellowi* where both sexes have a white eyebrow, and the sex on the label had to be trusted.

Song

Sound recordings of songs were obtained from 57 individuals (14 *B. m. cruralis*, 35 *B. m. sinensis*, 8 *B. m. goodfellowi*) (Additional file 1: Table S1; Fig. 1). We used both our own recordings and recordings from Xeno-canto (www.xeno-canto.org). Sonograms were produced and analysed in Avisoft-SASLab Pro 4.3 (Avisoft Bioacoustics, Berlin, Germany). First, we resampled the recordings at 22.05 kHz. Then, we created spectrograms with a fast Fourier transform length of 256 points, a hamming window with a frame size of 100% and an overlap of 50%, a frequency resolution of 86 Hz, and a time resolution 5.8 ms. We measured 15 strophes in sequence per individual, or all the strophes in a recording if fewer than 15 strophes for a certain individual. If a strophe had much background noise, we measured the next strophe instead. On average, we measured 7 ± 3 (mean \pm SD) strophes per individual. If a strophe had much background noise that affected measuring, we measured the next strophe instead. Strophes consist of elements (notes), and different strophes are separated from each other by pauses (>1 s). An element, which is the smallest unit measured, is defined as a continuous trace on a spectrogram.

For each strophe, we measured the duration, maximum frequency, minimum frequency, mean frequency, bandwidth, peak frequency, number of elements, number of distinct elements, element rate, maximum element duration, minimum element duration, maximum element bandwidth, minimum element bandwidth, duration of first element, duration of last element, peak frequency of first element, and peak frequency of last element. Element rate is number of elements in a strophe divided by duration of strophe. Peak frequency refers to frequency associated with the maximum energy. Mean frequency is the mean of maximum frequency and minimum frequency. Bandwidth is the difference between maximum frequency and minimum frequency. It was difficult to set a standard to measure the frequency of harmonics

which decrease gradually, so harmonic components were neglected. When measuring the maximum and minimum frequencies, “clicks” and “harsh” elements with gradual decrease in energy were neglected. Sometimes, there were several elements with relatively low energy at the end of a strophe, which could easily be obscured by background noise, especially in recordings with rather low quality; these elements were neglected. In total, 17 variables were measured, and all measurements were taken by the same person (C.X.).

We calculated average measurements for each individual, and used the means in the following analyses. We used a principal component analysis (PCA) with varimax rotation to compress the original variables into independent principal components (eigenvalues > 1) and then used a discriminant function analysis (DFA) to determine whether the songs of the three taxa could be distinguished. MANOVA was applied to assess overall differences between principal components of the different taxa, followed by independent sample *t* test for post hoc multiple comparisons. Analysis were carried out in SPSS Statistics version 20 (IBM Corp.).

Sonograms for publication were produced in Raven Pro 1.5 (Bioacoustics Research Program 2011), and songs used for sonograms were deposited in the Avian Vocalizations Center (AVoCet; <http://www.avocet.zoology.msu.edu>).

DNA

We obtained fresh DNA samples from 15 individuals (*7 B. m. cruralis*, *4 B. m. sinensis*, *4 B. m. goodfellowi*), as well as sequences from one additional *B. m. cruralis* from GenBank (Additional file 2: Table S2; Fig. 1). In the phylogenetic analyses, we also used previously unpublished sequences of *B. m. montana* and Lesser Shortwing (*B. leucophris carolinae*) and published sequences of Rusty-bellied Shortwing (*B. hyperythra*) (Additional file 2: Table S2).

DNA was extracted using QIA Quick DNEasy Kit (Qiagen, Inc.), according to the manufacturer’s instructions, but with 30 µl DTT added to the initial incubation step for the extraction from feathers. We sequenced the mitochondrial cytochrome *b* (*cytb*) and NADH dehydrogenase subunit 2 (ND2) genes and nuclear myoglobin intron 2 (myo) and ornithine decarboxylase introns 6–7 (ODC) according to the protocols described in Fregin et al. (2012).

Sequences were aligned and checked using Geneious 7.1.9 (Biomatters Ltd.). For the nuclear loci, heterozygous sites were coded as ambiguous. Substitution models were selected based on the Akaike Information Criterion calculated in jModeltest 2.1.7 (Darriba et al. 2012): GTR + Γ for *cytb*, HKY + Γ for ND2, HKY + I

for myo, and GTR + I for ODC. Trees were estimated by Bayesian inference using BEAST 1.8.4 (Drummond et al. 2012). Xml files were generated in the BEAST utility program BEAUti version 1.8.4 for the following analyses: myo and ODC separately; *cytb* + ND2; myo + ODC; and all loci combined. All but single-locus datasets were partitioned by locus, and all were analysed under the best-fit locus-specific model, a strict clock and a “birth-death incomplete sampling” tree prior with a normal distribution with mean 2.0 and standard deviation 1.0 for the growth rate. Default priors were used for the other parameters. Substitution and clock models were unlinked. The analysis was run for 500 million generations and sampled every 1000 generations.

In order to estimate divergence times, the *cytb* data set was analysed in BEAST version 1.8.4 (Drummond et al. 2012), with the same settings as for the concatenated data, except that we applied a strict clock with a normally distributed clock prior with a mean rate of 0.0105 substitutions/site/lineage/million years (my) and standard deviation 0.001, corresponding to a rate of 2.1%/my (Weir and Schlüter 2008).

Integrative species tree estimation was performed using *BEAST (Heled and Drummond, 2010) in BEAST 1.8.4, with gene trees and species trees estimated simultaneously. We ran analyses under the best-fit models, and a strict clock prior with the rate fixed to 1 (as per default). A piecewise linear population size model with a constant root was used as a prior for the multispecies coalescent and “birth-death incomplete sampling” as prior on divergence times. Default settings were used for the priors, except for the “birth-death mean growth rate”, for which a normal prior with initial value 1.0, mean 2.0 and standard deviation 1.0 was applied. 500 million generations were run, sampled every 1000 generations.

In all analyses, convergence to the stationary distribution of the single chains was inspected in Tracer 1.6 (Rambaut and Drummond 2014). The effective sample sizes (ESS) for the joint likelihood and other parameter values were > 300 (> 1000 for most parameters), representing good mixing of the MCMC. We also examined convergence and reproducibility by running each analysis three times, with random starting points. The first 10–25% of generations were discarded as “burn-in”, well after convergence was reached. Trees were summarized using TreeAnnotator version 1.8.4 (included in BEAST package), choosing “Maximum clade credibility tree” and “Mean heights”, and displayed in FigTree version 1.4.3 (Rambaut 2002). Xml files for all analyses and a tree file in Newick format for the *BEAST tree are available as Additional file 3: Material S1, Additional file 4: Material S2, Additional file 5: Material S3.

Results

Plumage and bare parts

Adult male

Adult male *B. m. cruralis* (Fig. 2b) is dark blue-grey (“blackish”) all over, with slightly paler grey belly to undertail-coverts, diffusely merging into blacker breast; the belly feathers have indistinct paler tips, often creating a faintly mottled appearance. The lores and uppermost throat are jet black, the latter diffusely merging with the slightly paler rest of the throat. The supercilium is pure white, usually largely concealed over/behind the eye except when excited.

Adult male *B. m. sinensis* (Fig. 2a) is overall considerably paler grey, with grey rather than black lores; the uppermost throat is often paler, rather than darker, than the rest of the throat; and the belly and undertail-coverts are often whitish. The legs are on average blacker in *B. m. cruralis* than in *B. m. sinensis*. No attempts were made to investigate whether there were additional differences within the UV spectrum, although it is unlikely that additional important differences would be discerned (cf. Vorobyev et al. 1998; Håstad and Ödeen 2008).

Brachypteryx m. goodfellowi (Fig. 2e) is sexually monomorphic, and adult male is “female-plumaged” (see below). Accordingly, adult male *B. m. goodfellowi* is very different from adult male *cruralis* and *sinensis* (and first-winter/-summer *sinensis*; see below).

Adult female

Adult female *B. m. cruralis* is uniformly dark brown above and on the ear-coverts (latter often with a buffish or rufous tinge), and with more rufous-brown edges to the uppertail-coverts, remiges and rectrices. The throat, breast and flanks are slightly paler brown (upper throat marginally paler, with a faint buffish tinge), diffusely merging with even paler belly and more rufous undertail-coverts. The lower forehead is diffusely rufous, and the supraloral and eye-ring are also rufous.

Adult female *B. m. sinensis* differs from adult female *B. m. cruralis* in lacking rufous on the forehead, lores and around the eye (just showing an indistinct pale buffish eye-ring); and in showing slightly paler throat and breast; whitish belly; and paler rufous-buff undertail-coverts. The base of the lower mandible appears to be rather pale in many *B. m. sinensis* as opposed to black in *B. m. cruralis*, and the legs paler than in *B. m. cruralis* (only observed on specimens, needs to be confirmed in the field).

Adult female (and adult male; see above) *B. m. goodfellowi* resembles adult female *B. m. cruralis*, but shows a prominent white supercilium (mostly concealed over/behind the eye when not excited); buffish-white belly; and paler rufous-buff undertail-coverts.

First-winter/-summer male

First-winter/-summer male *B. m. cruralis* (Fig. 2d, f) resembles adult female, but shows a white supercilium, which is usually concealed above/behind the eye, and mainly or entirely concealed also in front of the eye (but easily seen in the hand when feathers are parted). It can further be told from adult female by pale rufous edges and terminal spots/shaft-streaks to retained juvenile (outer) greater coverts (pale spots/shaft-streaks most distinct on innermost feathers; same pattern in first-winter/-summer female).

First-winter/-summer male *B. m. sinensis* (Fig. 2c) resembles adult male, but shows contrastingly browner retained juvenile remiges, primary coverts, alula and outer greater coverts, latter often with pale rufous/buffish spots on tips. Thus, first-winter/-summer *B. m. sinensis* is strikingly different from same-age male *B. m. cruralis*.

First-winter/-summer male *B. m. goodfellowi* presumably differs from adults (but not from first-winter/-summer female) by moult contrasts and pattern of retained juvenile greater coverts, but this has not been studied by us.

Morphometrics

Although *B. m. cruralis* and *B. m. sinensis* are similar in overall size, *B. m. cruralis* has the bill significantly longer and, in males, deeper than in *B. m. sinensis*; a shorter distance from carpal joint to tip of longest secondary but longer P1; shorter, more graduated (latter at least in females) tail that projects significantly less beyond the undertail coverts; and longer, heavier tarsus and longer hindclaw than *B. m. sinensis* (Table 1).

Factor scores of most individual *B. m. cruralis* and *B. m. sinensis* occupied taxon-exclusive morphospace, although there was overlap, and the small sample of *B. m. goodfellowi* fell out in the area of morphospace overlap (Fig. 3). By far the most important variables contributing to the differential loading of specimens of *B. m. cruralis* and *B. m. sinensis* on PC1 (Table 2) were a contrast between tail length plus projection of tail beyond undertail coverts (higher scores in *B. m. sinensis*) versus tarsus length (greater in *B. m. cruralis*). On both PC2 and PC3 (latter not graphed), wing length and tail graduation were the most important variables, but the taxa did not separate out well on these components. Within-taxon sexual variation was much less than that between *B. m. cruralis* and *B. m. sinensis* (Fig. 3).

Song

The song of *B. m. cruralis* (Fig. 4a, b) is a drawn-out (3.34 ± 0.78 s) thin, high-pitched (mean peak frequency 4.63 ± 0.38 kHz) ramble of notes of different pitch and

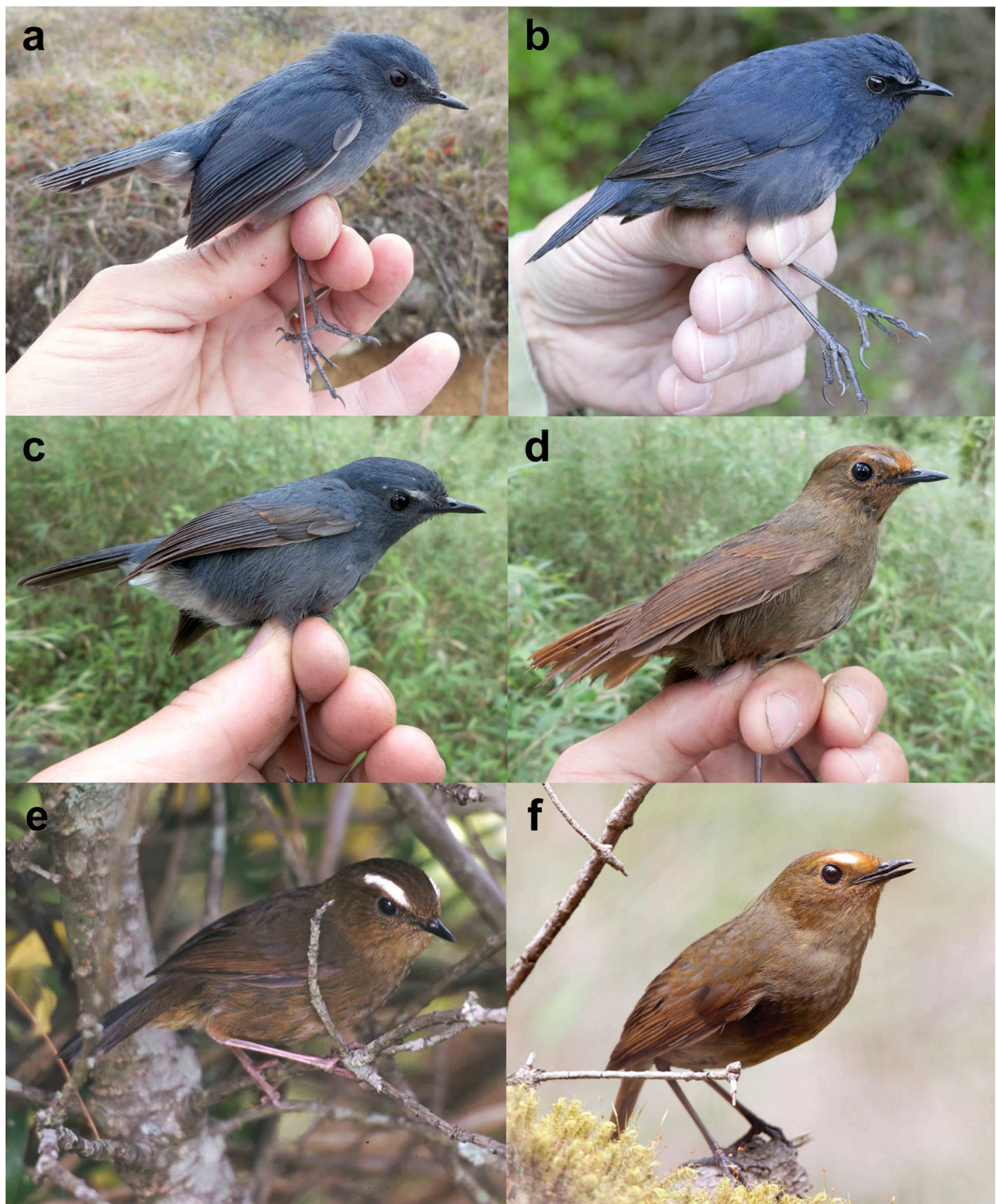


Fig. 2 **a** *Brachypteryx montana sinensis*, adult male, Wuyishan, Jiangxi, 25 April 2013 (IOZ 18252; AV 20015) (Per Alström); **b** *B. m. cruralis*, adult male, Dulongjiang, Yunnan, 5 May 2016 (IOZ 21894) (Per Alström); **c** *B. m. sinensis*, 1st-summer male, Wolong, Sichuan, 19 June 2015 (IOZ 20894; AV 20014) (Per Alström); **d** *B. m. cruralis*, 1st-summer male, Wolong, Sichuan, 19 June 2015 (IOZ 20893; AV 20012) (Per Alström); **e** *B. m. goodfellowi* Nantou county, Taiwan Island, 4 May 2004 (Chengte Yao); **f** *B. m. cruralis*, 1st-summer male, Jiuzhaigou, Sichuan, 14 May 2015 (Tang Jun/China Bird Tour)

Table 1 Univariate statistics for external measurements (mm) of skin specimens of *Brachypteryx montana cruralis*, *B. m. sinensis*, and *B. m. goodfellowi*

Variable	Males			Females		
	<i>cruralis</i>	<i>sinensis</i>	<i>goodfellowi</i>	<i>cruralis</i>	<i>sinensis</i>	<i>goodfellowi</i>
Culmen from skull	16.1 ± 0.4** (15.0–16.7, 13)	15.2 ± 0.7 (14.2–17.0, 20)	16.3 ± 0.5 (15.7–16.7, 3)	16.0 ± 0.8 ns (14.4–17.6, 22)	15.5 ± 0.8 (14.0–17.0, 18)	16.4 ± 0.5 (16.0–16.9, 3)
Culmen from feathers	11.8 ± 0.7** (11.0–12.0, 13)	10.7 ± 0.4 (10.0–11.4, 20)	11.2 ± 0.3 (11.0–11.5, 3)	11.7 ± 0.7* (10.5–12.9, 23)	10.9 ± 0.7 (10.1–13.0, 18)	11.5 ± 0.5 (11.4–11.6, 3)
Bill width	2.9 ± 0.2 ns (2.6–3.3, 13)	2.8 ± 0.3 (2.2–3.3, 22)	3.0 ± 0.2 (2.7–3.1, 3)	2.9 ± 0.2 ns (2.6–3.4, 24)	3.0 ± 0.2 (2.7–3.5, 18)	3.2 ± 0.2 (3.0–3.3, 3)
Bill depth	3.5 ± 0.2*** (3.3–3.8, 11)	3.1 ± 0.3 (2.6–3.8, 19)	3.2 ± 0.2 (3.0–3.3, 3)	3.4 ± 0.1 ns (3.2–3.6, 22)	3.3 ± 0.2 (3.1–3.6, 14)	3.4 ± 0.2 (3.2–3.5, 3)
Wing length	66.7 ± 2.2 ns (63.0–72.0, 13)	65.3 ± 1.6 (62.0–68.0, 22)	65.8 ± 1.8 (64.0–67.5, 3)	64.3 ± 2.0 ns (61.0–69.0, 27)	63.4 ± 2.3 (59.0–66.5, 21)	65.3 ± 4.7 (60.0–69.0, 3)
Secondary length	57.3 ± 2.9*** (53.0–62.0, 9)	63.3 ± 3.1 (58.0–67.0, 22)	60.3 ± 2.5 (58.0–63.0, 3)	55.7 ± 2.4*** (52.0–61.0, 15)	61.2 ± 2.8 (55.0–65.0, 21)	57.0 ± 4.4 (52.0–60.0, 3)
Primary projection	9.4 ± 1.3 ns (6.0–11.0, 13)	8.3 ± 2.0 (5.0–12.0, 22)	5.7 ± 0.6 (5.0–6.0, 3)	8.3 ± 1.1 ns (6.0–11.0, 27)	7.3 ± 1.9 (4.0–11.0, 21)	8.3 ± 0.6 (8.0–9.0, 3)
Primary 1 length	22.7 ± 1.1** (21.0–25.0, 13)	20.7 ± 1.5 (18.0–23.0, 22)	22.2 ± 1.3 (21.0–23.5, 3)	21.8 ± 1.7*** (19.0–25.0, 27)	19.9 ± 1.4 (24.0–30.0, 21)	21.0 ± 1.0 (20.0–22.0, 3)
Primary 1 shortfall	27.4 ± 1.8 ns (24.0–29.0, 13)	28.3 ± 1.6 (25.0–32.0, 22)	26.3 ± 1.2 (25.0–27.0, 3)	25.8 ± 2.1 ns (23.0–30.3, 26)	27.5 ± 1.8 (24.0–30.0, 21)	27.0 ± 2.0 (25.0–29.0, 3)
Primary 2 shortfall	11.9 ± 1.4 ns (9.0–14.0, 13)	12.1 ± 1.2 (10.0–14.0, 20)	12.7 ± 0.6 (12.0–13.0, 3)	11.5 ± 1.5 ns (9.0–15.0, 26)	11.4 ± 0.7 (10.0–13.0, 21)	13.0 ± 1.7 (12.0–15.0, 3)
Primary 3 shortfall	4.6 ± 0.9 ns (3.0–6.0, 13)	4.2 ± 0.8 (3.0–6.0, 22)	5.0 ± 1.0 (4.0–6.0, 3)	4.4 ± 1.1 ns (3.0–6.0, 26)	3.7 ± 0.6 (3.0–5.0, 21)	5.0 ± 1.0 (4.0–6.0, 3)
Primary 4 shortfall	1.4 ± 0.7 ns (0.0–2.0, 13)	1.3 ± 0.4 (1.0–2.0, 22)	1.7 ± 0.6 (1.0–2.0, 3)	1.1 ± 0.7 ns (0.0–3.0, 26)	0.9 ± 0.5 (0.0–2.0, 19)	1.5 ± 0.9 (0.5–2.0, 3)
Primary 5 shortfall	0.0 ± 0.0 ns (0.0–0.0, 13)	0.02 ± 0.1 (0.0–0.5, 22)	0.0 ± 0.0 (0.0–0.0, 3)	0.0 ± 0.0 ns (0.0–0.0, 26)	0.0 ± 0.0 (0.0–0.0, 19)	0.2 ± 0.3 (0.0–0.5, 3)
Tail length	43.7 ± 4.6** (34.3–49.2, 13)	48.8 ± 2.2 (45.7–52.3, 22)	47.9 ± 0.7 (47.4–48.7, 3)	42.3 ± 2.3*** (37.7–46.7, 27)	46.5 ± 1.8 (43.3–50.2, 21)	46.8 ± 2.5 (44.4–49.4, 3)
Tail graduation	5.8 ± 1.5 ns (3.0–8.0, 12)	4.0 ± 1.6 (0.0–6.0, 20)	7.0 ± 1.0 (6.0–8.0, 3)	5.5 ± 1.6* (3.0–9.0, 26)	4.1 ± 1.3 (2.0–7.0, 20)	8.0 ± 1.0 (7.0–9.0, 3)
Undertail coverts to tail tip	18.9 ± 3.2*** (13.0–24.0, 13)	25.2 ± 1.9 (22.0–29.0, 22)	23.7 ± 0.6 (23.0–24.0, 3)	18.6 ± 2.3*** (15.0–24.0, 27)	22.3 ± 1.8 (18.0–26.0, 21)	22.7 ± 2.1 (21.0–25.0, 3)
Tarsus length	31.5 ± 1.3*** (29.3–34.7, 12)	27.7 ± 0.8 (26.3–29.2, 22)	30.2 ± 1.6 (28.3–31.2, 3)	30.9 ± 1.1*** (28.4–32.9, 27)	27.5 ± 0.9 (25.8–29.3, 21)	31.6 ± 2.4 (29.8–34.3, 3)
Tarsus distal width	3.1 ± 0.1*** (2.9–3.3, 13)	2.8 ± 0.8 (2.1–3.0, 22)	2.9 ± 0.1 (2.8–3.0, 3)	3.1 ± 0.1*** (2.8–3.5, 27)	2.9 ± 0.1 (2.7–3.1, 13)	3.0 ± 0.1 (2.9–3.1, 3)
Hindclaw length	7.9 ± 0.5*** (6.3–8.5, 13)	7.0 ± 0.4 (6.3–7.7, 22)	7.1 ± 0.2 (6.8–7.3, 3)	7.5 ± 0.4*** (6.7–8.3, 26)	6.8 ± 0.4 (6.1–7.7, 21)	7.3 ± 0.2 (7.1–7.5, 3)

Measurements are presented as mean ± SD (range, n). Significance tests (two-sample t-tests: ns = Bonferroni-adjusted p value > 0.05; * = p ≤ 0.05, ** = p ≤ 0.01, *** = p ≤ 0.001) are shown between male *B. m. cruralis* and male *B. m. sinensis* (under male *cruralis*) and between female *B. m. cruralis* and female *B. m. sinensis* (under female *cruralis*)

duration, which give the song an “undulating” quality; it often sounds as if it is delivered during one long exhalation, with the end trailing off. The strophes are separated by long pauses, usually at least 6 s. Individual males have large repertoires, and strophes are usually not repeated two or more times in succession.

The song of *B. m. sinensis* (Fig. 4c–e) is markedly different, consisting of much shorter (0.83 ± 0.09 s), on average lower-pitched (mean peak frequency 3.93 ± 0.37 kHz) strophes, which usually have shorter pauses in between

(usually 3–8 s). Each strophe is sometimes given several times in succession, before switching to another strophe type. Individual males have large repertoires.

The song of *B. m. goodfellowi* (Fig. 4f, g) sounds superficially similar to that of *B. m. sinensis*, mainly because it consists of short, fairly simple strophes. However, analyses of sonograms reveal quite different syntax and pattern, although these differences are difficult to quantify. It usually begins with a drawn-out note and often ends with a short series of rather brief, often complex, notes

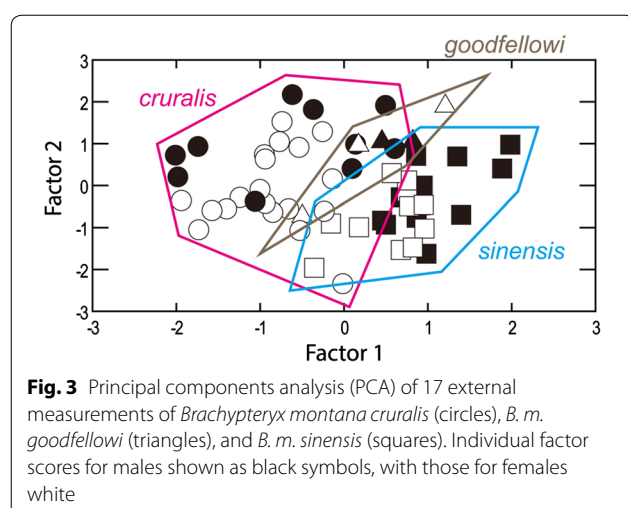


Table 2 Summary results of principal components analysis (PCA) of external measurements of *Brachypteryx montana cruralis*, *B. m. sinensis*, and *B. m. goodfellowi* (individual PC I and PC II scores graphed in Fig. Y)

Component loadings	PC I	PC II	PC III
External measurement			
Culmen from skull	-0.27	0.17	0.16
Culmen from feathers	-0.35	0.14	0.09
Bill width	0.07	-0.01	0.01
Bill depth	-0.07	0.06	0.04
Wing length	0.69	1.35	-1.32
Primary projection	-0.68	0.46	-0.38
Primary 1 length	-0.66	0.07	-0.36
Primary 1 shortfall	0.95	0.87	-0.68
Primary 2 shortfall	0.38	0.82	0.16
Primary 3 shortfall	0.02	0.47	0.29
Primary 4 shortfall	0.08	0.19	0.04
Primary 5 shortfall	0.01	0.02	0.00
Tail length	3.39	0.52	0.62
Tail graduation	-0.30	1.22	1.24
Undertail coverts to tail tip	2.96	-0.69	0.09
Tarsus length	-1.37	0.69	0.63
Tarsus distal width	-0.13	0.05	0.01
Hind claw length	-0.29	0.15	0.01
Eigenvalues	24.881	6.52	4.96
% Total variance explained	48.97	12.83	9.77

The most important loadings on each factor are shown in italics

of alternating pitch that is given two or sometimes three times (one or a few simple, drawn-out notes are often given after the initial note, and very thin, faint notes are often given at the very end). In *B. m. sinensis*, there is often an alternation between drawn-out and shorter

notes, and repeated series of shorter notes are less common. However, in *B. m. sinensis*, repetitions of single notes multiple times are common, as well as “rolling” drawn-out notes (with “serrated edges” in sonograms), unlike in *B. m. goodfellowi*. In our sample of *B. m. goodfellowi*, repetition of the same strophe twice in succession was exceptional.

In the PCA of songs, four components with eigenvalues >1 were extracted from the data set (Table 3). PC1 was positively correlated with duration, number of elements, number of different elements, maximum frequency, bandwidth, maximum element bandwidth, peak frequency of first element, and negatively correlated with minimum frequency; PC2 was positively correlated with minimum element duration, peak frequency of last element, and negatively correlated with rate; PC3 was negatively correlated with minimum element bandwidth; PC4 was positively correlated with maximum element duration, duration of first element (Table 3). A plot of PC1 versus PC2 revealed three clusters with partial overlap (Fig. 5). *Brachypteryx m. cruralis* was largely separated from the others on PC1, and *B. m. goodfellowi* from the others on PC2. The following principal components differed among the taxa (MANOVA: Pillai’s Trace = 1.555, $F_{8,102} = 44.496$, $p < 0.001$). PC1 was significantly different among all taxa ($p < 0.019$); *B. m. goodfellowi* was significantly different from *B. m. cruralis* and *B. m. sinensis* on PC2 ($p < 0.001$), while the two latter taxa were not significantly different on PC2 ($p = 0.243$); *B. m. cruralis* was significantly different from *B. m. goodfellowi* and *B. m. sinensis* on PC3 ($p < 0.002$), while the two latter taxa were not significantly different on PC3 ($p = 0.077$). PC4 was not significantly different among the taxa ($p > 0.133$).

The DFA correctly classified 96.4% of the individuals based on the original song measurements and 94.7% based on the mean measurements of all strophes for each individual (Table 4). 100% of the *B. m. cruralis* were correctly identified, whereas 2.9% of the *B. m. sinensis* were mis-classified as *B. m. goodfellowi* and 12.5% of the *B. m. goodfellowi* were mis-classified as *B. m. sinensis*.

DNA

All analyses of combined mitochondrial and nuclear loci supported a sister relationship between *B. m. sinensis* and *B. m. goodfellowi*, with *B. m. cruralis* being sister to these (Fig. 6). The tree based on the two mitochondrial genes was topologically identical to the combined tree, but with lower support (0.89) for the clade comprising the three focal taxa (Additional file 6: Fig. S2). The tree based on the two nuclear introns combined as well as single-locus analyses of the introns supported *cruralis* and *goodfellowi* as monophyletic (0.95–1.00) but failed to recover *sinensis* as monophyletic (Additional file 6: Fig.

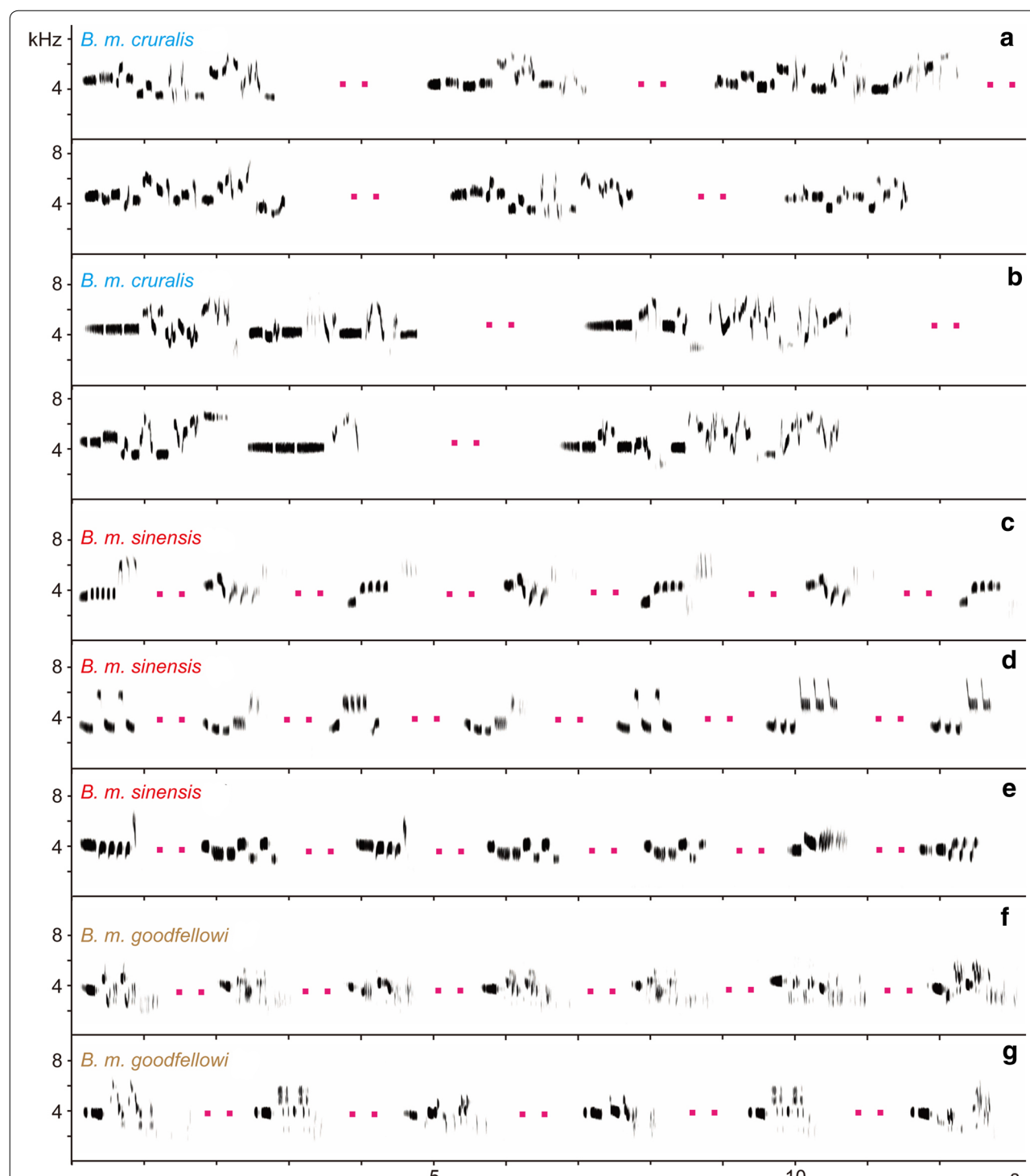
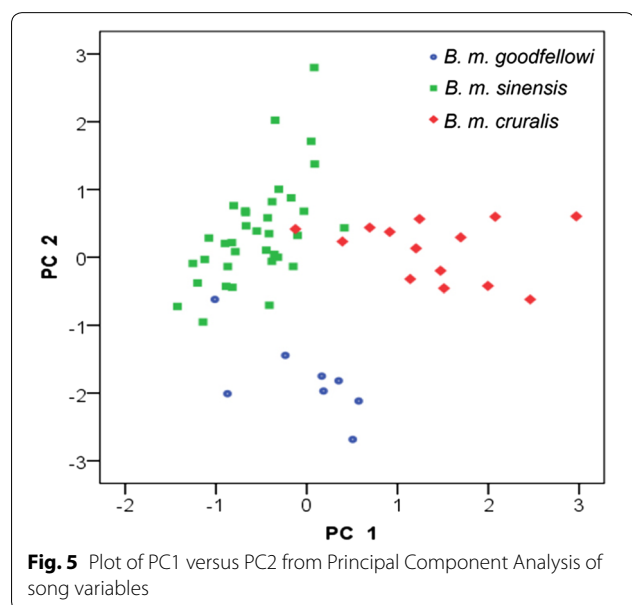


Fig. 4 Sonograms of songs of **a** *Brachypteryx montana cruralis*, Singalila National Park, West Bengal, India, 2600 m, 29 May 1997 (Per Alström; AV 20010); **b** *B. m. cruralis*, Wolong, Sichuan Province, China, May 1990 (Per Alström; AV 20011); **c** *B. m. sinensis*, Wolong, Sichuan Province, China, 2860 m, 19 June 2015 (IOZ 20894; AV 20014) (Per Alström); **d** *B. m. sinensis*, Foping, Shaanxi Province, China, 2160 m, 8 June 2011 (IOZ 16361; AV 20013) (Per Alström); **e** *B. m. sinensis*, Wuyishan, Jiangxi Province, China, 2060 m, 25 April 2013 (IOZ 18252; AV 20015) (Per Alström); **f** *B. m. goodfellowi*, Dasyueshan Forest Reserve, Taiwan Island, China, 2600 m, 25 April 2009 (XC34156) (Frank Lambert); **g** *B. m. goodfellowi*, Dasyueshan Forest Reserve, Taiwan Island, China, 2100 m, 24 April 2009 (XC34261) (Frank Lambert). The coloured dots indicate artificially shortened pauses between strophes

Table 3 Principal component analysis of song variables of *Brachypteryx montana cruralis*, *B. m. sinensis*, and *B. m. goodfellowi*

	PCA1	PCA2	PCA3	PCA4
Duration of strophe (s)	0.879	-0.003	0.348	0.192
Number of elements in strophe	0.880	-0.176	0.357	0.100
Number of distinct elements in strophe	0.898	-0.069	0.332	0.109
Rate	-0.003	-0.852	0.093	-0.272
Maximum frequency of strophe (Hz)	0.828	0.337	0.348	0.039
Minimum frequency of strophe (Hz)	-0.706	0.525	0.284	-0.197
Mean frequency (Hz)	0.467	0.630	0.510	-0.066
Bandwidth (Hz)	0.947	0.048	0.157	0.113
Peak frequency of strophe (Hz)	0.327	-0.106	0.681	0.353
Maximum element duration (s)	0.438	0.087	0.013	0.850
Minimum element duration (s)	-0.311	0.759	-0.367	-0.025
Maximum element bandwidth (Hz)	0.901	0.012	-0.038	0.153
Minimum element bandwidth (Hz)	-0.337	-0.069	-0.725	0.289
Duration of first element (s)	0.044	0.051	0.002	0.931
Duration of last element (s)	0.438	0.614	-0.107	0.338
Peak frequency of first element (Hz)	0.753	-0.131	0.387	0.151
Peak frequency of last element (Hz)	-0.136	0.777	0.283	-0.189
Eigenvalue	6.751	3.15	2.22	2.185
% Variance explained	39.713	18.529	13.061	12.852

**Fig. 5** Plot of PC1 versus PC2 from Principal Component Analysis of song variables

S2). The split between *B. m. sinensis* and *B. m. goodfellowi* was dated to 4.1 million years ago (mya; 95% highest posterior distribution [HPD] 2.8–5.5 mya), in the mid-Pliocene, and between these two and *B. m. cruralis* to 5.8 mya (95% HPD 4.1–7.5 mya), in the late Miocene (Fig. 6). The analyses also found *B. m. montana*, *B. leucophrys carolinae* and *B. hyperythra* to form a clade, with a sister relationship and divergence time of 3.9 mya (95% HPD 2.7–5.2 mya) between the two former (although not strongly supported in all analyses) (Fig. 6; Additional file 6: Fig. S2).

Geographical distributions

Brachypteryx m. cruralis and *B. m. sinensis* were previously considered widely disjunct, with the former distributed from the central Himalayas to central China and northern Thailand and southern Vietnam, and the latter restricted to Guizhou, Guangxi, Hunan, Jiangxi, Fujian and southern Shaanxi Provinces in southeast China (e.g. Cheng 1987; Collar 2005). However, in mid-June 2015, we found two singing males of *B. m. sinensis* in sympatry with *B. m. cruralis* at 2860–2870 m in Wolong Nature Reserve in Sichuan Province, China (Figs. 1, 2, 4, 6). One male *B. m. sinensis* and one male *B. m. cruralis* apparently had overlapping territories, as both were attracted to the same spot by playback of their own song, but did not show any response to the other taxon's song. We have also examined one sound recording by Mike Nelson (XC265947) of a *B. m. sinensis* from Wolong, at 1600 m in late May. *Brachypteryx m. cruralis* is fairly common in Wolong. *Brachypteryx m. goodfellowi* is endemic to Taiwan Island (Fig. 1).

Discussion

Brachypteryx montana cruralis, *B. m. sinensis* and *B. m. goodfellowi* differ congruently in adult and first-winter/summer plumage and song, and their genetic divergences are substantial, with estimated divergences in the late Miocene to mid-Pliocene. Kyriazis et al. (2018) found even deeper divergence between *B. m. cruralis* and *B. m. sinensis* than we did (> 9 mya). The difference between our estimate and the one by Kyriazis et al. (2018) is likely due to the use of different loci and different molecular clock calibrations. We note that the most recent common ancestor for the five taxa in our study (6.99 mya) is very similar to that estimated for the common ancestor of *B. montana cruralis*, *B. leucophrys* and *B. hyperythra* (7.15 mya) in the study of Himalayan songbirds by Price et al. (2014) using multiple fossil calibrations (*sinensis* and *goodfellowi* not analysed). The divergences among the three continental taxa are rather close to or considerably deeper than among *B. m. montana* from Java, *B. leucophrys carolinae* and *B. hyperythra*. There are also

Table 4 Discriminant function analysis of song variables of *Brachypteryx montana cruralis*, *B. m. sinensis*, and *B. m. goodfellowi*

Species	Predicted group membership			Total
	<i>goodfellowi</i>	<i>sinensis</i>	<i>cruralis</i>	
Cross-validated ^a				
Count				
<i>goodfellowi</i>	7	1	0	8
<i>sinensis</i>	1	33	0	34
<i>cruralis</i>	0	0	14	14
%				
<i>goodfellowi</i>	87.5	12.5	0.0	100.0
<i>sinensis</i>	2.9	97.1	0.0	100.0
<i>cruralis</i>	0.0	0.0	100.0	100.0

^a Each individual was assigned to a taxon on the basis of discriminant functions calculated from all individuals' songs in the dataset except the one being classified

differences in sexual dimorphism between the three taxa (*B. m. goodfellowi* being monomorphic, unlike the two others) and male plumage maturation (first-winter/-summer male *B. m. cruralis* being "female-like", unlike same-age male *B. m. sinensis*). We also detected statistically significant differences in structure between *B. m. cruralis* and *B. m. sinensis*, although these overlap; *B. m. goodfellowi* is intermediate in morphometrics, although our sample size of the latter is too small to test statistically (all taxa had overlapping clusters in the PCA). Moreover, we have found *B. m. cruralis* and *B. m. sinensis* in sympatry in the breeding season in Sichuan Province, China, with seemingly overlapping territories, but no evidence of intertaxon territoriality. Taken together, these facts suggest that all three taxa should be treated as separate species.

Our suggestion to treat *B. m. cruralis*, *B. m. sinensis* and *B. m. goodfellowi* as three different species is in agreement with the treatment by del Hoyo and Collar (2016), which was based on differences between the two former in plumage ("score 6" according to their scoring system) and song ["rather longer, more warbled (at least 1)" in *cruralis*]; and differences between *B. goodfellowi* and the two others in plumage (especially sexual monomorphism: "score 4") and "notably longer bill" ("score 2"), but no difference in song (in total "score 8"). While we concur that plumage differences are pronounced between all three taxa, our measurements (Table 1) do not bear out the statement by del Hoyo and Collar (2016) that the bill is notably longer in *B. m. goodfellowi* than in *B. m. cruralis*, and a larger sample of *B. m. goodfellowi* would likely show it to be similar in bill length to *B. m.*

cruralis and that both are significantly longer-billed than *B. m. sinensis*.

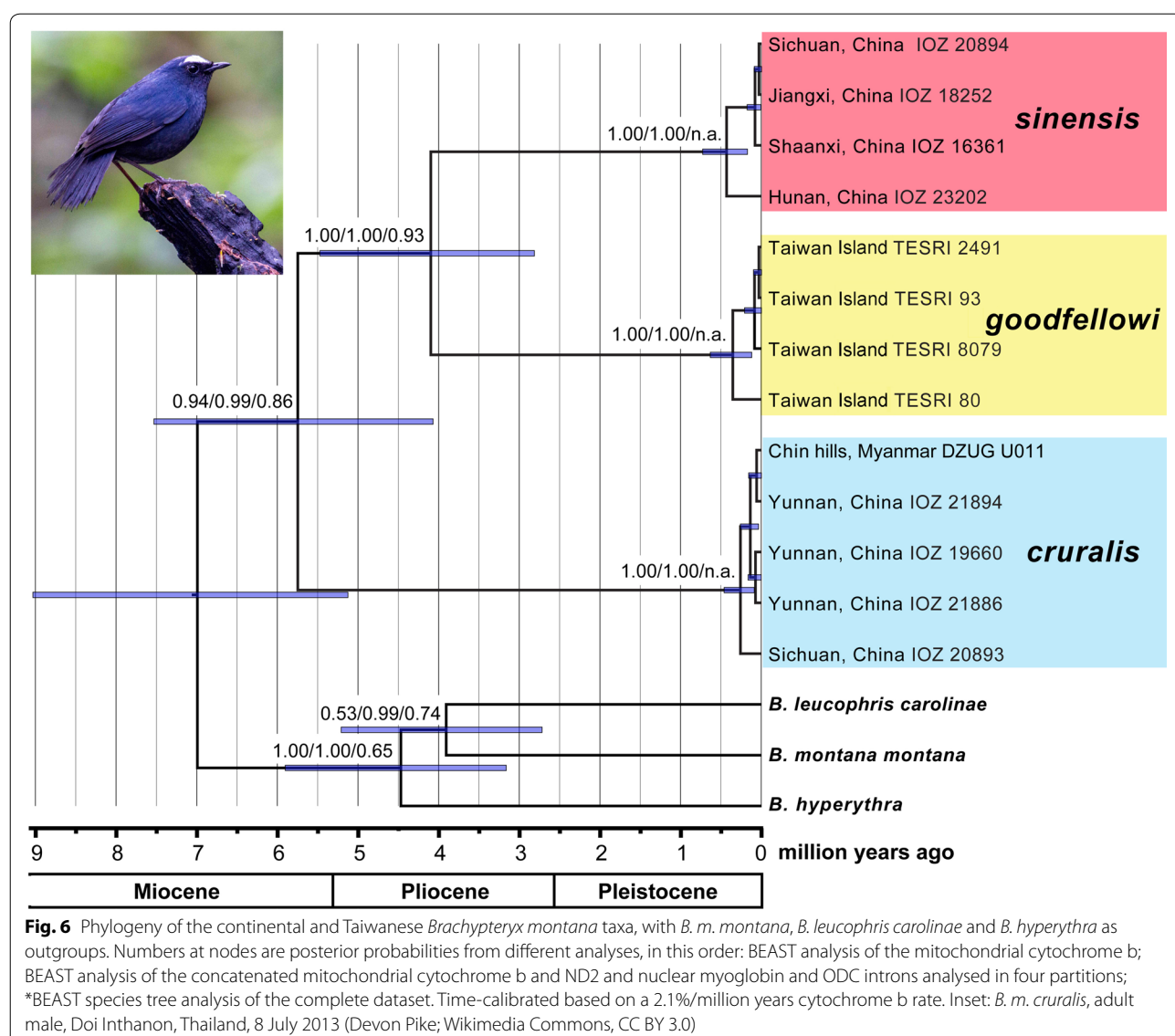
The present study does not analyse the Philippine and Indonesian taxa in this complex, but all of those that have recently been suggested to be different species, including Javan *B. m. montana*, are at least as different-looking from the three mainland and Taiwanese taxa as these are from each other (del Hoyo and Collar 2016; Eaton et al. 2016). Moreover, the ancient divergence between the tree continental/Taiwanese taxa and *B. m. montana*, and the fact that *B. leucophrys*, which is sympatric with both *B. m. cruralis* and *B. m. sinensis*, is more closely related to *B. m. montana* than *B. m. montana* is to *B. m. cruralis* and *B. m. sinensis*, support splitting the tree continental/Taiwanese taxa from *B. m. montana*. In other words, the two Asian mainland species should be referred to as *B. cruralis* and *B. sinensis*, and the Taiwanese one as *B. goodfellowi*. del Hoyo and Collar (2016) proposed the English names Himalayan Shortwing for the first, Chinese Shortwing for the second, and Taiwanese Shortwing for the third.

Clement and Rose (2015) stated that first-winter/-summer ("first-year") male *B. cruralis* has "blue bases (underlying olive-brown tips) to crown, nape and upperparts, to inner webs of wing-coverts and flight and tail feathers, which become progressively deeper blue on head and upperparts". This strongly disagrees with our experience, though it seems to match some adult females. Moreover, the white supercilium, which distinguishes first-winter/-summer male from females of all ages, is not mentioned in their main text, but is shown on the plate and mentioned in the caption to the same.

We note that in males, *B. sinensis* has the fastest plumage maturation, as the first-winter/-summer plumage is adult-like, whereas it takes one additional year for *B. cruralis* to reach adult plumage. In contrast, *B. goodfellowi* never obtains a distinct male plumage, and might be considered paedomorphic.

Conclusion

We agree with a recent suggestion based exclusively on studies of morphology and songs (del Hoyo and Collar 2016) that the two continental Asian and single Taiwanese taxa in the *Brachypteryx montana* complex are better treated as three distinct species, which are specifically different from *B. montana* sensu stricto: *B. cruralis*, *B. sinensis* and *B. goodfellowi*. This is based on concordant differences in morphology, songs and DNA, as well as sympatry in the breeding season between the two continental taxa.



Additional files

Additional file 1: Table S1. Original data for sound recordings of songs of *B. m. cruralis*, *B. m. sinensis* and *B. m. goodfellowi*.

Additional file 2: Table S2. Samples used for phylogenetic analyses, including GenBank accession numbers.

Additional file 3: Material S1. BEAST analysis of cytochrome b for dating (Fig. 6).

Additional file 4: Material S2. BEAST analysis of all loci, concatenated (Additional file 6: Fig. S1).

Additional file 5: Material S3. *BEAST analysis of all loci (Fig. 6).

Additional file 6: Fig. S1. Phylogeny of the continental and Taiwanese *Brachypteryx montana* taxa, with *B. m. montana*, *B. leucophrys carolinae* and *B. hyperythra* as outgroups, based on BEAST analysis of the mitochondrial cytochrome b and ND2 and nuclear myoglobin and ODC introns analysed in four partitions. Includes three *cruralis* samples not included in Fig. 1 due to missing sequences. **Fig. S2.** Trees inferred by BEAST based on cytb and ND2 (**a**) and myo and ODC (**b**), each dataset analysed in two partitions; and single-locus analyses of myo (**c**) and ODC (**d**).

Authors' contributions

PA, PCR, YL, FL and UO designed the study; PA, PCR, MG, YL, MZ, CZ, JZ, CY, JAE, RH and UO collected data; MG, GC, MZ, YH and UO generated DNA sequences; PA, PCR and CX analysed the data; PA, PCR and YL made the figures; PA, PCR and CX wrote the first draft. All authors read and approved the final manuscript.

Author details

¹ Department of Ecology and Genetics, Animal Ecology, Evolutionary Biology Centre, Uppsala University, Norbyvägen 18D, 752 36 Uppsala, Sweden. ² Swedish Species Information Centre, Swedish University of Agricultural Sciences (SLU), Box 7007, 750 07 Uppsala, Sweden. ³ Key Laboratory of Zoological Systematics and Evolution, Institute of Zoology, Chinese Academy of Sciences, Beijing 100101, China. ⁴ Department of Integrative Biology and MSU Museum, Michigan State University, East Lansing, MI 48864, USA. ⁵ Bird Group, The Natural History Museum at Tring, Akeman Street, Tring HP23 6AP, UK. ⁶ Ministry of Education Key Laboratory for Biodiversity and Ecological Engineering, College of Life Sciences, Beijing Normal University, Beijing 100875, China. ⁷ Gothenburg Natural History Museum, Box 7283, 402 35 Göteborg, Sweden. ⁸ State Key Laboratory of Biocontrol, Department of Ecology, School of Life Sciences, Sun Yat-sen University, Guangzhou 510275, China. ⁹ University of Chinese Academy of Sciences, Beijing 100049, China. ¹⁰ Cloud Mountain Conservation,

Dali 671003, Yunnan, China.¹¹ High-Altitude Experimental Station, Endemic Species Research Institute, COA, Chi-chi 55244, Taiwan, China.¹² Birdtour Asia, 17 Keats Avenue, Littleover, Derby DE23 4EE, UK.¹³ Department of Biology and Environmental Sciences, Systematics and Biodiversity, University of Gothenburg, Box 463, 405 30 Göteborg, Sweden.

Acknowledgements

Staff of the following museums (alphabetical by acronym) provided access to the specimens that form the basis for the morphological analyses: Paul Sweet and Joel Cracraft, American Museum of Natural History (AMNH), New York; Nate Rice, Academy of Natural Sciences (ANS) of Drexel University, Philadelphia; Robert Prys-Jones and Mark Adams of The Natural History Museum (BMNH-UK), Tring, UK; John Bates and Ben Marks, Field Museum of Natural History (FMNH), Chicago; Jeremiah Trimble, Museum of Comparative Zoology (MCZ), Harvard University; Janet Hinshaw, University of Michigan Museum of Zoology (UMMZ), Ann Arbor; and Helen James and Chris Milensky, the National Museum of Natural History (USNM), Smithsonian Institution, Washington, DC. We gratefully acknowledge valuable comments from two anonymous reviewers.

Competing interests

The authors declare that they have no competing interests.

Availability of data and materials

Most of the data analysed for this study are included in this published article or in its supplementary material. Additional material can be obtained from the corresponding author.

Consent for publication

Not applicable.

Ethics approval and consent to participate

The study fulfils ethical requirements.

Funding

P.A. gratefully acknowledges Jornvall Foundation, Mark and Mo Constantine, and the Chinese Academy of Sciences Visiting Professorship for Senior International Scientists (No. 2011T2S04), and P.A. and U.O. acknowledge the Swedish Research Council (Grant Nos. 2015-04402 and 2015-04651, respectively).

Received: 8 May 2018 Accepted: 10 October 2018

Published online: 30 October 2018

References

- Bioacoustics Research Program. Raven Pro: Interactive sound analysis software (version 1.5). Ithaca, New York: Cornell Lab of Ornithology; 2011.
- Cheng T-H. A synopsis of the avifauna of China. Beijing: Science Press; 1987.
- Clement P, Rose C. Robins and chats. London: Christopher Helm; 2015.
- Collar NJ. 2005. Family Turdidae (thrushes). In: J. del Hoyo et al., editors. Handbook of the birds of the world, vol. 10. Cuckoo-shrikes to Thrushes. Barcelona: Lynx Edicions. p. 514–807.
- Darriba D, Taboada GL, Doallo R, Posada D. jModelTest 2: more models, new heuristics and parallel computing. Nat Methods. 2012;9:772.
- del Hoyo J, Collar NJ. HBW and BirdLife international illustrated checklist of the birds of the world. Volume 2: Passerines. Barcelona: Lynx Edicions; 2016.
- Dickinson EC, Christidis L (eds). The Howard & Moore complete checklist of the birds of the world. Vol. 2 Passerines. Fourth edition. Eastbourne: Aves Press; 2014.
- Drummond AJ, Suchard MA, Xie D, Rambaut A. Bayesian phylogenetics with BEAUTI and the BEAST 1.7. Mol Biol Evol. 2012;29:1969–73.
- Eaton JA, van Balen B, Brickle NW, Rheindt FE. Birds of the Indonesian Archipelago. Greater Sundas and Wallacea. Barcelona: Lynx Edicions; 2016.
- Fregin S, Haase M, Olsson U, Alström P. New insights into family relationships within the avian superfamily Sylvioidea (Passeriformes) based on seven molecular markers. BMC Evol Biol. 2012;12:157.
- Gill F, Donsker D (eds). IOC world bird list (v 8.1). <http://www.worldbirdnames.org>. 2018. <https://doi.org/10.14344/IOCML.8.1>.
- Håstad O, Ödeen A. Different ranking of avian colors predicted by modeling of retinal function in humans and birds. Am Nat. 2008;171:831–8.
- Heled J, Drummond AJ. Bayesian inference of species trees from multilocus data. Mol Biol Evol. 2010;27:570–80.
- Kyriazis CC, Alam B, Wjodyla M, Hackett S, Hosner P, Mays HI Jr, Heaney LR, Reddy S. Colonization and diversification of the white-browed shorthwing (Aves: Muscicapidae: *Brachypteryx montana*) in the Philippines. Mol Phylogenet Evol. 2018;121:121–31.
- Price TD, Hooper DM, Buchanan CD, Johansson US, Tietze DT, Alström P, Olson U, Ghosh-Harihar M, Ishtiaq F, Gupta SK, Martens JE, Harr B, Singh P, Mohan D. Niche filling slows the diversification of Himalayan songbirds. Nature. 2014;509:222–5.
- Rambaut A. Figtree 1.4.0. <http://tree.bio.ed.ac.uk/software/figtree/>; 2002.
- Rambaut A, Drummond AJ. TreeAnnotator (version 1.8.1). <http://beast.bio.ed.ac.uk>; 2014.
- Rasmussen PC, Anderton JC. Birds of South Asia: the Ripley guide. Barcelona: Lynx Edicions; 2005.
- Robin WV, Vishnudas CK, Gupta P, Rheindt FE, Hooper DM, Ramakrishnan U, Reddy S. Two new genera of songbirds represent endemic radiations from the Shola Sky Islands of the Western Ghats, India. BMC Evol Biol. 2017;17:31.
- Sangster G, Alström P, Forsmark E, Olsson U. Multilocus phylogenetic analysis of Old World chats and flycatchers reveals extensive paraphyly at family, subfamily and genus level (Aves: Muscicapidae). Mol Phylogenet Evol. 2010;57:380–92.
- Vorobyev M, Osorio D, Bennett ATD, Marshall NJ, Cuthill IC. Tetrachromacy, oil droplets and bird plumage colours. J Comp Physiol A. 1998;183:621–33.
- Weir JT, Schlüter D. Calibrating the avian molecular clock. Mol Ecol. 2008;17:2321–8.
- Zuccon D, Ericson PGP. A multi-gene phylogeny disentangles the chat-flycatcher complex (Aves: Muscicapidae). Zool Scr. 2010;39:213–24.

Ready to submit your research? Choose BMC and benefit from:

- fast, convenient online submission
- thorough peer review by experienced researchers in your field
- rapid publication on acceptance
- support for research data, including large and complex data types
- gold Open Access which fosters wider collaboration and increased citations
- maximum visibility for your research: over 100M website views per year

At BMC, research is always in progress.

Learn more biomedcentral.com/submissions

